

# ANALYSIS OF DYNAMIC SHEAR BANDS UNDER COMBINED LOADING

R.C. BATRA and LIDUN WANG

*Department of Mechanical and Aerospace Engineering and Engineering Mechanics  
University of Missouri-Rolla, Rolla, Mo 65401-0249 USA*

## ABSTRACT

We study dynamic plane strain thermomechanical deformations of a thermally softening viscoplastic body of square cross-section and loaded in combined compression and shear at a nominal strain-rate of approximately 5000/s. A material defect in the body is simulated by adding a temperature bump centered at the centroid of the cross-section to the otherwise uniform initial temperature. By varying the ratio of the compressive to shear loading, we study five different problems. It is found that in each case a shear band initiates from the centroid and propagates in the direction of maximum shearing. The equivalent nominal strain at which a shear band develops is highest for the case of simple shearing and least for the case of simple compression.

## 1. INTRODUCTION

Even though shear bands were first observed by Tresca [1] in 1878 and by Massey [2] in 1921 during the hot forging of a metal bar, the research activity in this field has picked up since 1944 when Zener and Hollomon [3] observed 32  $\mu\text{m}$  wide shear bands during the punching of a hole in a steel plate. They postulated that the heat produced due to plastic deformations softened the material which became unstable when this softening exceeded its hardening due to strain and strain-rate effects. The instability eventually resulted in the localization of the deformation into one or more narrow bands of intense plastic deformation usually called shear bands since the predominant mode of deformation within the band is shearing. These bands are called adiabatic since there is not enough time for the heat produced within the band to be conducted away, at least during the early stages of its development. However, during the final growth of the band, heat conduction probably controls its width because of the development of steep temperature gradients across the band. Here we account for the inertia forces, heat conduction, thermal softening, strain-rate hardening, and the heat generated due to plastic working, and seek an approximate solution of the initial-boundary-value problem by the finite element method. The set of coupled stiff ordinary differential equations obtained from the governing partial differential equations by using the Galerkin method are integrated with respect to time by using the IMSL subroutine LSODE.

For references to the related work, the reader is referred to two recent books [4, 5] and to review articles [6-7] on the subject. We note that nearly all of the previous work [8-21] that dealt with the analysis of the dynamic problem is numerical, and none of it considered combined loading. Since most practical problems involve complex loadings, it seems worthwhile to study the initiation and growth of shear bands under combined compressive and shear loads.

## 2. FORMULATION OF THE PROBLEM

We use an updated Lagrangian description of motion to study plane strain deformations of a viscoplastic body of square cross-section, and use rectangular Cartesian coordinates (cf. Fig. 1) with origin at its centroid to describe deformations of the body. In order to solve for the deformations of the body at time  $t + \Delta t$ , we take its configuration at time  $t$  as the reference configuration but do not assume that the intervening deformations are infinitesimal. Equations governing deformations of the body and written in terms of the referential description are

$$(\rho J) \dot{\phantom{x}} = 0, \quad (2.1)$$

$$\rho_0 \dot{v}_i = T_{i\alpha,\alpha}, \quad (2.2)$$

$$\rho_0 \dot{e} = -Q_{\alpha,\alpha} + T_{i\alpha} v_{i,\alpha} \quad (2.3)$$

where  $\rho$  is the mass density of a material particle in the present configuration at time  $t + \Delta t$ ,  $\rho_0$  its mass density in the reference configuration at time  $t$ ,  $J = \rho_0/\rho$  equals the determinant of the deformation gradient  $F_{i\alpha} = x_{i,\alpha}$ ,  $x_i$  gives the

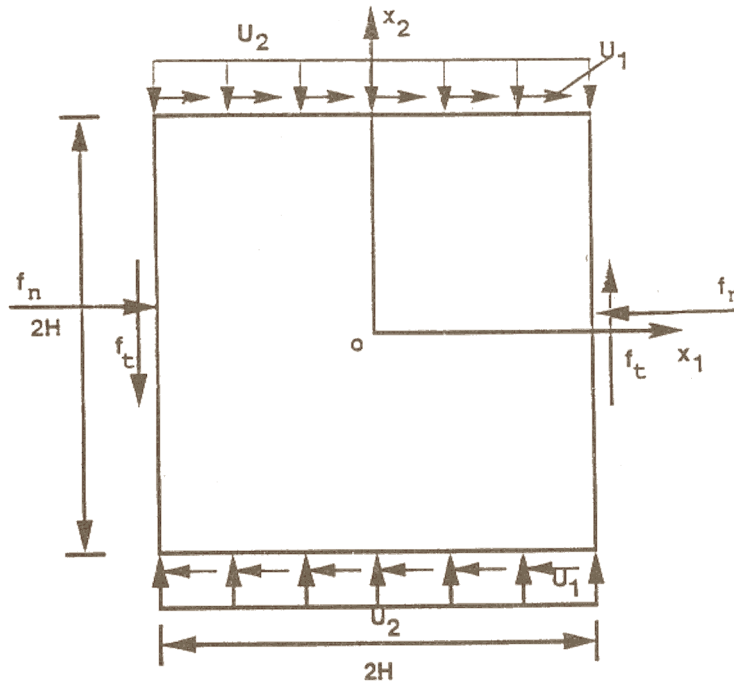


Figure 1. A schematic sketch of the problem studied.

present position of a material particle that occupied place  $X_\alpha$  in the reference configuration, a superimposed dot indicates the material time derivative,  $v_i$  is the velocity of a material particle,  $T_{i\alpha}$  is the first Piola-Kirchhoff stress tensor, a comma followed by  $\alpha$  ( $i$ ) indicates partial derivative with respect to  $X_\alpha$  ( $x_i$ ); a repeated index implies summation over the range of the index,  $e$  is the internal energy per unit mass, and  $Q_\alpha$  is the heat flux per unit area in the reference configuration. We assume that  $x_3 = 0$  is the plane of deformation, and the indices  $i$  and  $\alpha$  range over 1, 2. Equations (2.1), (2.2), and (2.3) express, respectively, the balance of mass, balance of linear momentum, and the balance of internal energy. These need to be supplemented by constitutive relations, initial conditions, and boundary conditions.

Previous experimental [23] and numerical [10-21] works have indicated that the material within the band is severely deformed and the temperature and strain-rate within the band are quite high too. Constitutive relations that describe well the response of the material over such wide ranges of strains, strain-rates, and temperatures have not been established yet. For the simple shearing problem, Batra and Kim [11] have shown that various constitutive relations, namely, those due to Litonski [24], Bodner and Partom [25], Johnson and Cook [26], Wright and Batra [15], and the power law [27] give similar qualitative but different quantitative results. It is highly unlikely that any one of these material models is valid under conditions prevailing within the band. Nevertheless, we here use the one proposed by Batra [28] who generalized to three dimensional deformations that suggested by Litonski for simple shearing deformations. Batra and co-workers [18-21] have used it to study the initiation and growth of shear bands in different problems. We assume that the following constitutive relations describe well the material response over the range of conditions likely to occur during the shear banding process.

$$\sigma_{ij} = -p(\rho) \delta_{ij} + 2\mu D_{ij}, \quad (2.4)$$

$$T_{i\alpha} \equiv (\rho_0/\rho) X_{\alpha,j} \sigma_{ij}, \quad (2.5)$$

$$2\mu = [\sigma_0 / (\sqrt{3}I)] (1 - \nu\theta) (1 + bI)^m, \quad (2.6)$$

$$2D_{ij} = v_{i,j} + v_{j,i}, \quad (2.7)$$

$$2I^2 = \tilde{D}_{ij} \tilde{D}_{ji}, \quad \tilde{D}_{ij} = D_{ij} - (1/3) D_{kk} \delta_{ij}, \quad (2.8)$$

$$p(\rho) = B(\rho/\rho_r - 1), \quad (2.9)$$

$$Q_\alpha = -k(\rho_0/\rho) X_{\alpha,i} \theta_{,i}, \quad (2.10)$$

$$\rho_0 \dot{e} = \rho_0 c \dot{\theta} + \rho_0 \dot{p}(\rho) / \rho^2. \quad (2.11)$$

Here  $\sigma_{ij}$  is the Cauchy stress tensor,  $\sigma_0$  the yield stress in a quasistatic isothermal simple compression or tension test conducted at the room temperature,  $p$  the hydrostatic pressure determined by the equation of state (2.9) in which  $B$  may be

identified as the bulk modulus and  $\rho_r$  is the mass density in the stress-free reference configuration,  $\underline{D}$  is the strain-rate tensor,  $\tilde{D}$  its deviatoric part,  $\nu$  equals the coefficient of thermal softening, material parameters  $b$  and  $m$  describe the strain-rate sensitivity of the material,  $c$  is the specific heat and  $k$  equals the thermal conductivity of the material. The material parameters  $b$ ,  $m$ ,  $c$ ,  $k$ ,  $K$ , and  $B$  are taken to be independent of the temperature. Equation (2.10) is the Fourier law of heat conduction written in the referential description, and equation (2.4) may be interpreted as representing a non-Newtonian fluid whose viscosity  $\mu$  depends upon the temperature and strain-rate. In terms of the deviatoric stress tensor  $\underline{s}$ , defined by

$$s_{ij} = \sigma_{ij} + [p - (2/3) \mu D_{kk}] \delta_{ij} \quad (2.12)$$

$$= 2 \mu \tilde{D}_{ij} \quad (2.13)$$

equation (2.4) when combined with equations (2.6) and (2.8), can be written as

$$[(1/2) (s_{ij} s_{ji})]^{1/2} = [\sigma_0/\sqrt{3}] (1 - \nu \theta) (1 + bI)^m. \quad (2.14)$$

Equation (2.14) is the kinetic equation of state and may also be viewed as a generalized von-Mises yield criterion that accounts for the decrease of the flow stress with the temperature rise and its increase with the increase in strain-rate. Here we have not accounted for the strain-hardening of the material in order to reduce the number of variables to be considered. Wang and Batra [13] studied the effect of kinematic hardening on the initiation and growth of shear bands and found that the qualitative nature of results remained unaffected. They also showed that, for the plane strain compression problem, the constitutive relation proposed by Brown, Kim, and Anand [29] gave results similar to those obtained by using equation (2.4). Bell [30], Lindholm and Johnson [31], and Lin and Wagoner [32] have observed the affine dependence of the flow stress upon the temperature rise. However, the range of temperatures examined by these investigators is not as large as that likely to occur in the shear band problem. Chen and Batra [33] used the foregoing constitutive relations in studying the penetration of an aluminum target by a steel rod, and found that the computed depth of penetration matched well with the test values. We note that Zienkiewicz et al. [34] have used a constitutive relation akin to equation (2.4) to study an extrusion problem.

For the boundary conditions we take

$$v_1 = \pm U_1(t), \quad v_2 = \mp U_2(t), \quad Q_2 = 0 \text{ on } X_2 = \pm H, \quad (2.15)$$

$$n_i T_{i1} = f_n(t), \quad e_i T_{i1} = f_t(t), \quad Q_1 = 0 \text{ on } X_1 = \pm H, \quad (2.16)$$

where  $U_1$  and  $U_2$  are prescribed functions of time  $t$ ,  $\underline{n}$  is an outward unit normal and  $\underline{e}$  is a unit tangent vector to a bounding surface. The boundary conditions (2.15) and (2.16) imply that all bounding surfaces are thermally insulated, the tangential and normal components of velocity are prescribed on the top and bottom surfaces, and on the left and right surfaces time dependent normal and shearing tractions are applied. We note that without these tractions, the left and right surfaces will very likely not stay straight. That normal tractions may develop in nonlinear materials deformed in simple shear follows from several examples given in Truesdell and Noll's book [36]. The values of  $f_n(t)$  and  $f_t(t)$  are computed from the solution of the problem at time  $(t - \Delta t)$ . We consider loadings such that

$$U_2(t) = \alpha U_1(t), \quad (2.17)$$

$$U_1(t) = \begin{cases} v_0 t / (0.005 H) & t \leq 0.005 H / v_0, \\ v_0 & t \geq 0.005 H / v_0, \end{cases} \quad (2.18)$$

where  $v_0$  is the steady value of the prescribed speed. We analyze the problem for  $\alpha = 0, 0.5, 1.0, 2.0$  and  $\infty$ ; the first case corresponds to simple shearing and the last one to pure compression. For  $\alpha = \infty$ ,  $U_1 = 0$  and  $U_2$  is given by equation (2.18).

The initial conditions considered are

$$\rho(\underline{x}, 0) = \rho_r, \quad \underline{v}(\underline{x}, 0) = \mathbf{0}, \quad \theta(\underline{x}, 0) = \varepsilon (1 - r^2)^9 \exp(-5r^2),$$

$$r^2 = X_1^2 + X_2^2. \quad (2.19)$$

That is, the body is initially at rest, is stress-free, has uniform mass density, and the initial temperature is high in a small region around the centroid of the cross-section. The value of  $\varepsilon$  in equation (2.19) models, in some sense, the strength of the defect.

### 3. COMPUTATIONAL CONSIDERATIONS

Substitution from the constitutive relations (2.4) through (2.11) into the balance laws (2.1)-(2.3) results in coupled nonlinear partial differential equations which along with initial conditions (2.19) and boundary conditions (2.15) and (2.16) are to be solved for  $\rho$ ,  $\mathbf{v}$  and  $\theta$ . These nonlinear partial differential equations are first reduced to a set of coupled nonlinear ordinary differential equations by using the Galerkin approximation [35] and the lumped mass matrix. The square cross-section in the stress free reference configuration is discretized into  $30 \times 30$  uniform square elements, with each square then divided into two triangles, and the coordinates of node points are updated after every time step. Thus the finite element mesh does not consist of uniform elements after the body has been deformed. Also, the sides of triangular elements are not necessarily aligned along the eventual direction of the shear band. Needleman [37] has pointed out that finite element meshes designed so that element sides in the deformed configuration are aligned along the band give sharper bands. The lumped mass matrix is obtained by using the row-sum technique [35]. At each node, the mass density, the temperature, and two components of velocity are to be determined after every time step. The coupled nonlinear stiff ordinary differential equations are integrated by using the Gear method [38] incorporated in the subroutine LSODE taken from the package ODEPACK developed by Hindmarsh [39]. The subroutine adjusts the time step adaptively until a solution of the coupled nonlinear stiff ordinary differential equations has been computed to the desired accuracy. The finite element code developed earlier by Batra and Liu [18] was modified to study the present problem.

### 4. COMPUTATION AND DISCUSSION OF RESULTS

We assigned following values to various material and geometric parameters in order to compute results.

$$\begin{aligned} b &= 10,000 \text{ s}, \quad \sigma_0 = 333 \text{ MPa}, \quad k = 49.22 \text{ Wm}^{-1} \text{ }^\circ\text{C}^{-1}, \quad m = 0.025, \\ c &= 473 \text{ J kg}^{-1} \text{ }^\circ\text{C}^{-1}, \quad \rho_r = 7860 \text{ kg m}^{-3}, \quad B = 128 \text{ GPa}, \\ H &= 5 \text{ mm}, \quad v_0 = 25 \text{ ms}^{-1}, \quad \nu = 0.0222 \text{ }^\circ\text{C}^{-1} \end{aligned} \quad (4.1)$$

Except for the value of the thermal softening coefficient  $\nu$ , these values are for a typical hard steel. The value of the thermal softening coefficient  $\nu$  is intentionally taken to be large in order to reduce the CPU time required for the band to fully develop. It should not affect the qualitative nature of results. The rather high value of the thermal softening coefficient results in material softening due to its being heated up because of plastic working in overcoming the strain-rate hardening of the material at a low value of the average strain. We note that Batra and Liu [18] used the foregoing values (4.1) and 9-noded quadrilateral elements to analyze the initiation and development of shear bands in a viscoplastic body. However, their initial conditions corresponded to the situation when initial transients had died out.

The results below are discussed in terms of the following non-dimensional variables indicated by a superimposed bar.

$$\bar{s} = s/\sigma_0, \quad \bar{\theta} = \theta/\theta_0, \quad \bar{x} = x/H, \quad \bar{I} = HI/v_0, \quad \bar{t} = tv_0/H, \quad \bar{v} = v/v_0 \quad (4.2)$$

where  $\theta_0 = \sigma_0/(\rho_r c) = 89.6 \text{ }^\circ\text{C}$  (4.3)

Henceforth, we use non-dimensional variables only and drop the superimposed bars.

Figure 2 depicts the effective stress  $s_e$ , defined as the right-hand side of equation (2.14), versus the average strain  $\gamma_{\text{avg}}$  given by

$$\gamma_{\text{avg}} = \sqrt{\left(\frac{\dot{\gamma}}{H}\right)^2 + \left(\frac{U_2}{H}\right)^2} \quad (4.4)$$

for homogeneous deformations of the block with  $\alpha = 0, 1$  and  $\infty$ . In this set of computations, the initial temperature was taken to be uniform. It is clear that the effective stress attains its peak value when the average strain equals about 8% for each one of the three cases.

In Fig. 3 we have plotted the evolution, at the centroid of the cross-section, of the second invariant  $I$  of the deviatoric strain-rate tensor for the five cases studied. If we associate the initiation of the shear band with the instant when  $I$  begins to increase sharply then the shear band initiates at the largest value of  $\gamma_{\text{avg}}$  for the case of simple shearing and at the least value of  $\gamma_{\text{avg}}$  when the block is deformed in simple compression. The value of  $\gamma_{\text{avg}}$  at the instant of the initiation of the shear band gradually decreases with an increase in the value of  $\alpha$ , i.e., with an increase in the vertical component of the prescribed velocity. Due to the large temperature perturbation introduced at the centroid, the band initiates before the peak in the effective stress is attained for  $\alpha = 2$  and  $\infty$ . We note that the average strain-rate equals  $5000 \text{ s}^{-1}$  for  $\alpha = 0$  and  $\infty$  but

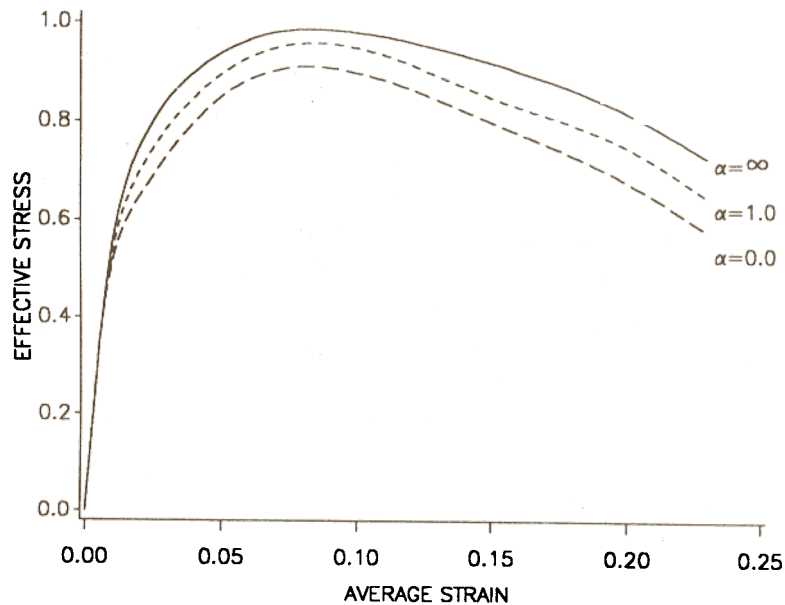


Figure 2. Effective stress vs. average strain for homogeneous deformations of the block with  $\alpha = 0, 1$  and  $\infty$ .

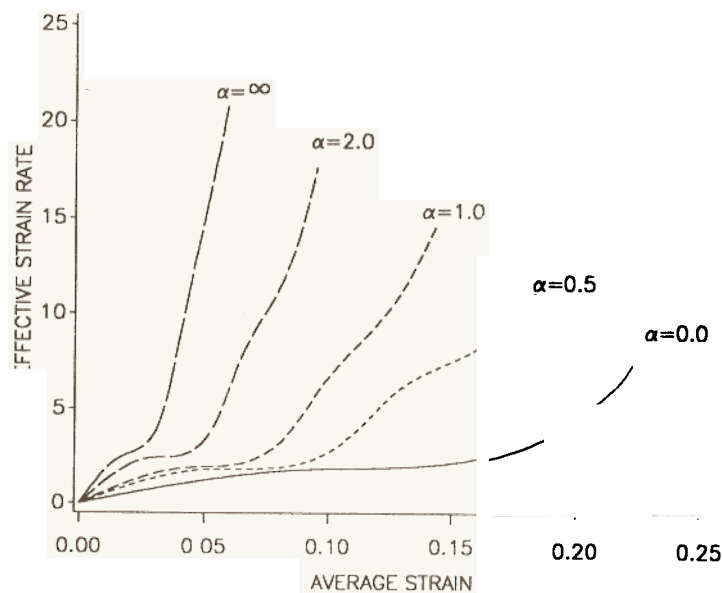


Figure 3. Evolution of the second invariant of the deviatoric strain-rate tensor at the centroid of the cross-section.

is higher for the other three cases studied. However, because of the low strain-rate sensitivity, it does not affect noticeably the homogeneous stress-strain curve (cf. Fig. 2) and the value of  $\gamma_{avg}$  when the effective stress attains its maximum value. We note that Batra and Ko [41] found that the initiation of a shear band was considerably delayed in a viscoplastic block deformed in axisymmetric compression as compared to that when it was deformed in plane strain compression. Thus the state of deformation at a material point seems to affect significantly the value of  $\gamma_{avg}$  at which a shear band will initiate.

The computations were stopped when one of the triangular elements had been severely distorted so as to make the jacobian of the mapping from the master right-handed triangular element to it negative. One could rezone the deformed area to compute results for subsequent deformations of the body or use the adaptive mesh refinement technique developed by Batra and Ko [40]. This was deemed to be beyond the scope of the present investigation.

The evolution of the temperature at the block center, shown in Fig. 4, reveals that the rate of increase of temperature is highest when the block is deformed in simple compression and least when it is deformed in simple shear. Also, once a shear band has initiated the temperature rises sharply when the body is being deformed in simple compression and rather

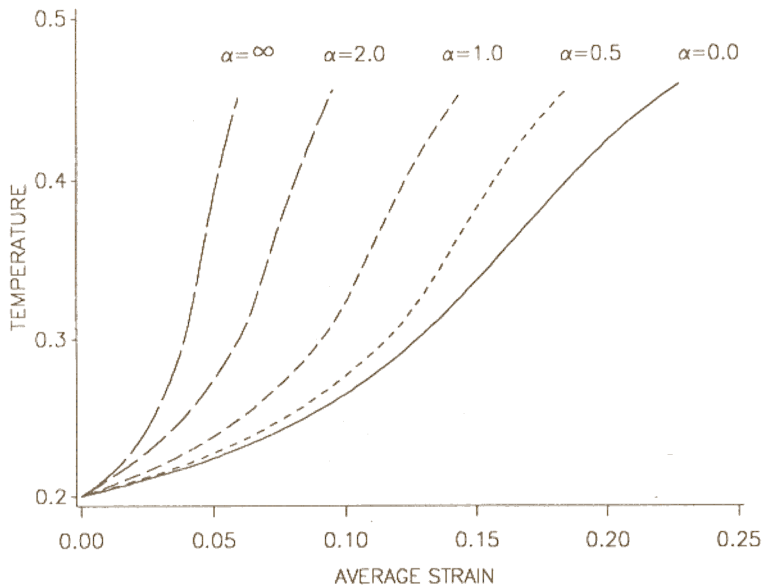


Figure 4. Evolution of the temperature at the centroid of the cross-section.

gradually for the case of simple shearing deformations of the body. The rate of increase of temperature both prior to and subsequent to the initiation of a shear band increases with an increase in the value of  $\alpha$ . The plot of the effective stress at the block center vs. the average strain there given in Fig. 5 reveals that the effective stress decreases most rapidly when the block is deformed in simple compression and quite slowly when it is deformed in simple shear. This is to be expected because the rather low value of  $m$  means that the magnitude of  $I$  has less noticeable effect on the value of the effective stress which being an affine function of temperature drops with an increase in the value of the temperature at the block center. We note that the normal and shearing tractions applied on the left and right surfaces to keep them straight were found to be of the order of  $10^{-2}$ .

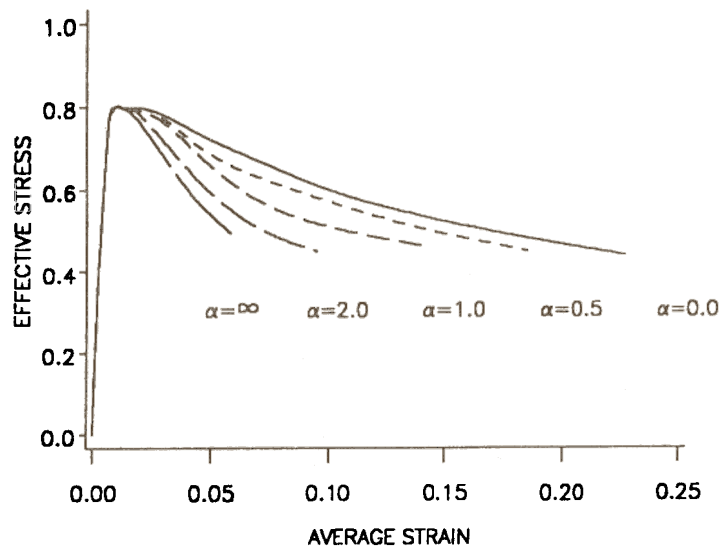


Figure 5. Evolution of the effective stress at the centroid of the cross-section.

For the axisymmetric compression problem Batra and Ko [41] found that the temperature at the block center rather than the nominal or average strain there was a better indicator of when a shear band initiates. In order to see whether or not such a correlation exists in the present problem, we have plotted in Fig. 6 the variation of the second invariant  $I$  of the deviatoric strain-rate tensor at the block center versus the temperature there. Except when the block is deformed in simple shear, the curves for the other four cases look alike. However, it is hard to decipher from them when a shear band initiates in earnest.

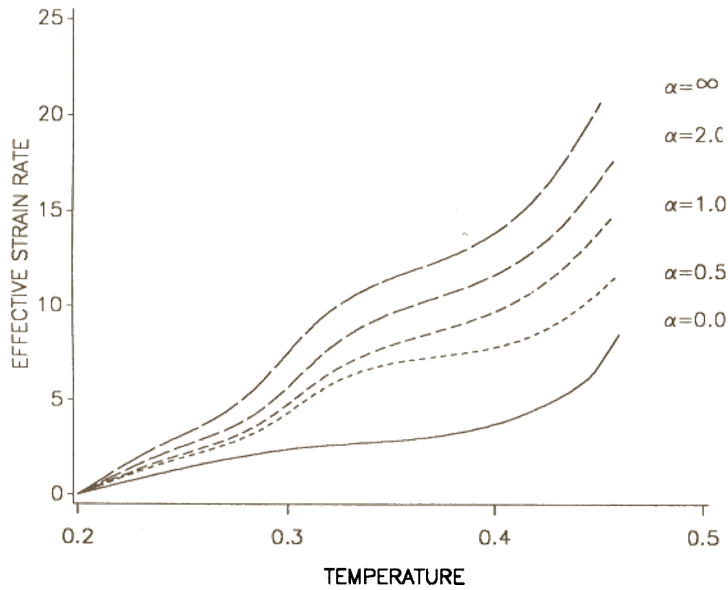


Figure 6. Variation of the second invariant of the deviatoric strain-rate tensor at the centroid of the cross-section vs. the temperature there.

In an attempt to delineate the development of a shear band within the body, we have plotted in Fig. 7 contours of the second invariant  $I$  of the deviatoric strain-rate tensor at  $\gamma_{avg} = 0.085, 0.097, 0.133$  and  $0.143$ . The loading corresponds to  $\alpha = 1$ , i.e., the block is compressed and sheared simultaneously at the same rate. The contours are plotted in the reference configuration. It is apparent that contours of successively increasing values of  $I$  originate at the centroid of the cross-section and propagate outwards in the direction of maximum shearing. The orientation of the band in the reference configuration does not change with time. Also, the severely deforming region does not narrow down too much because of the rather coarse mesh used. That the orientation of the band depends upon  $\alpha$  should be evident from Fig. 8 wherein are shown contours of  $I$  at the late stage of the band development for the five loadings studied. It is clear that the inclination of the band with the horizontal line increases with an increase in the value of  $\alpha$  and equals the maximum value of  $45^\circ$  for the case of simple compression. For  $\alpha = 0.5, 1$  and  $2$ , the band makes an angle, measured clockwise from the horizontal, of  $14.7^\circ, 22.3^\circ$ , and  $37.4^\circ$  respectively. The requirement that the top and bottom surfaces stay flat precludes the formation of two bands except in the case of simple compression in which case two bands aligned along the main diagonals form.

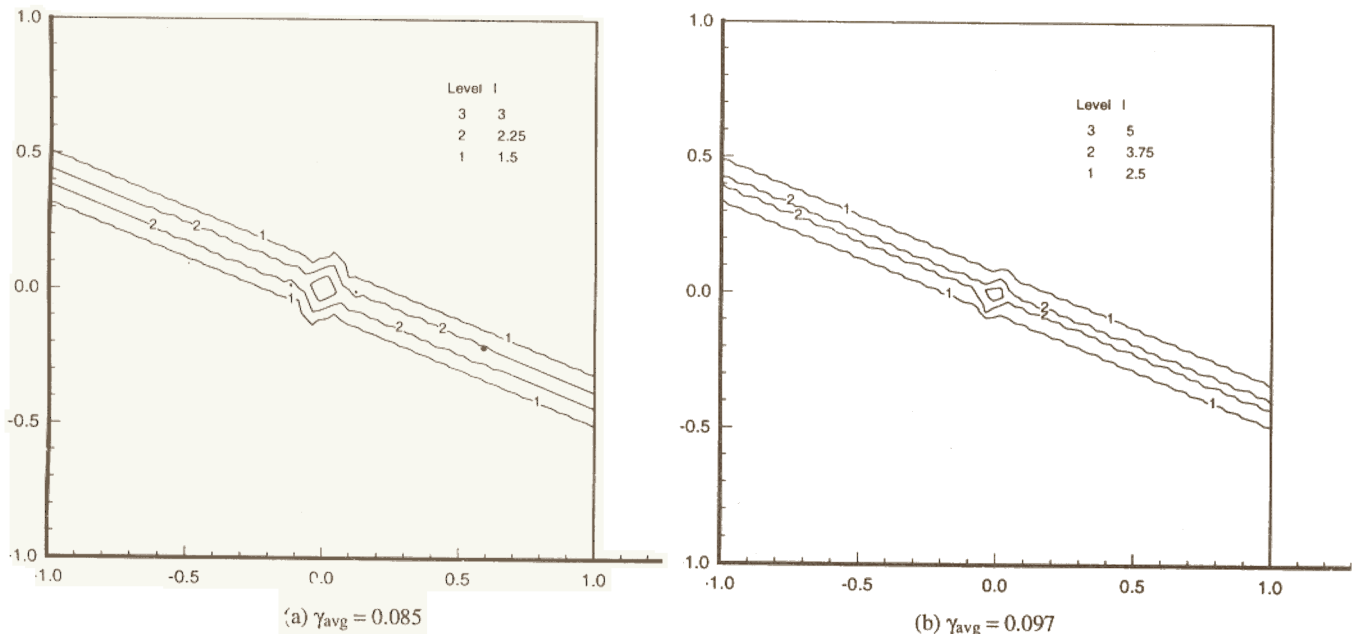
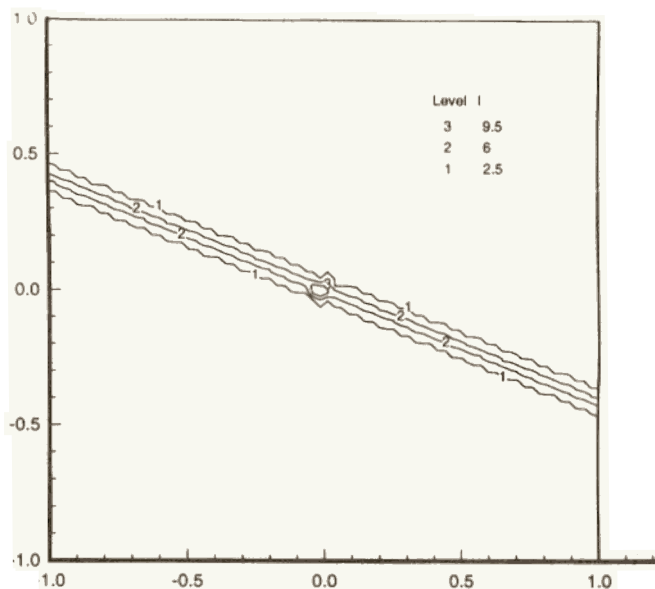
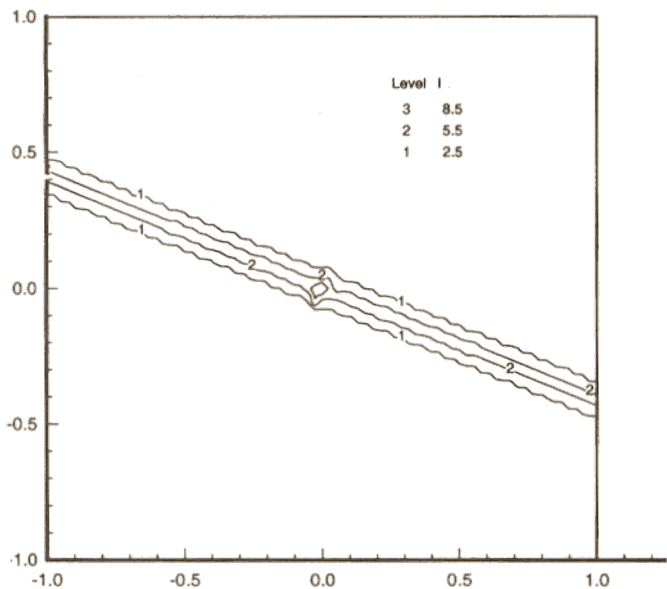


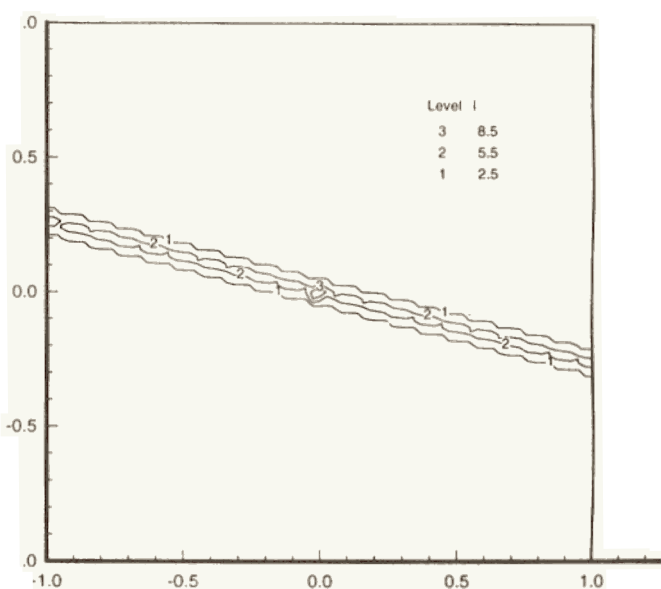
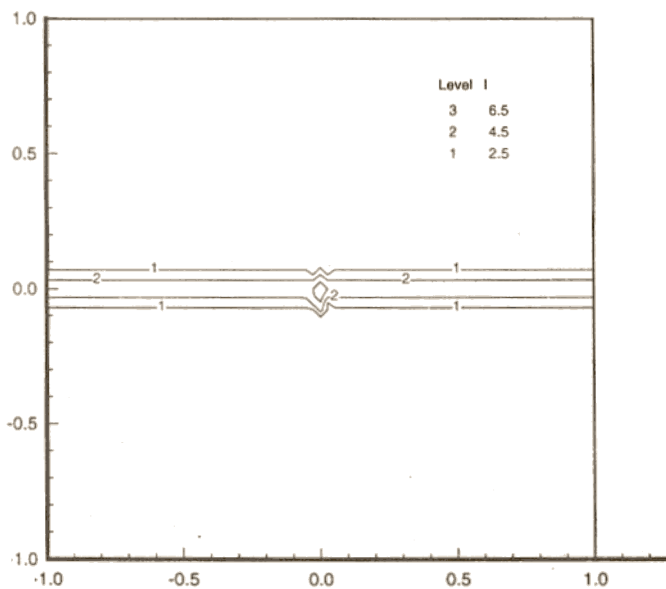
Figure 7



(c)  $\gamma_{avg} = 0.133$ , (d)  $\gamma_{avg} = 0.143$   
 Figure 7. Contours of the second invariant  $I$  of the deviatoric strain-rate tensor for  $\alpha =$

For  $\alpha = 0.5, 1, 2$ , and  $\infty$  the  $y$ -component of velocity and for  $\alpha = 0$  the  $x$ -component of the velocity distribution within the deforming region at a late stage of the band development is plotted in Fig. 9. These plots illustrate that the deforming region is divided into several zones separated by the shear band across which the velocity field jumps by a finite amount. It supports Tresca's [1] and Massey's [2] assertions that the tangential velocity is discontinuous across a shear band. In our work, the velocity field is required to be continuous.

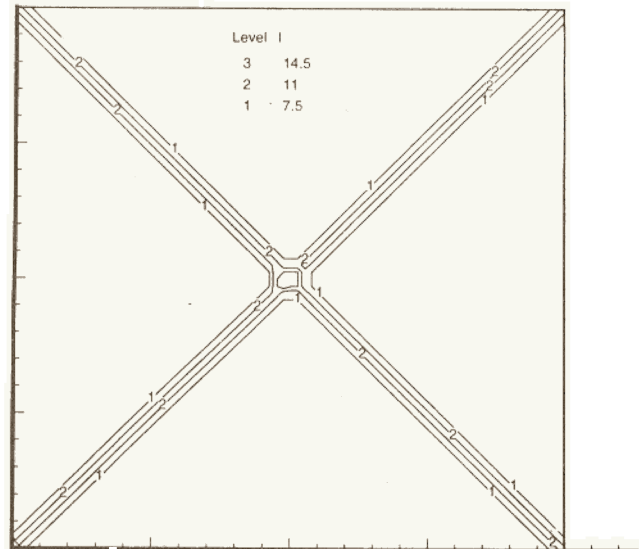
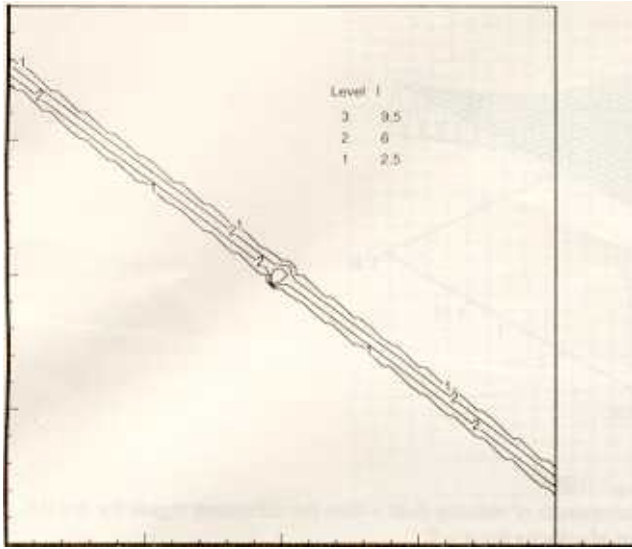
The change in the orientation of the shear band with  $\alpha$  is confirmed by the plots of the deformed mesh shown in Fig. 10 at the late stage of the band formation. The deformed mesh plotted consists of quadrilateral elements obtained by joining two adjacent triangular elements. These plots evince that essentially one element on either side of the band centerline is severely deformed. A finer mesh could not be used because of the limitations on the core storage and the CPU time available for the project.



(a)  $\alpha = 0.0, \gamma_{avg} = 0.227$

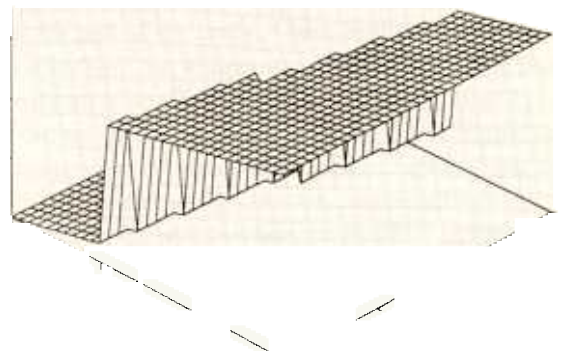
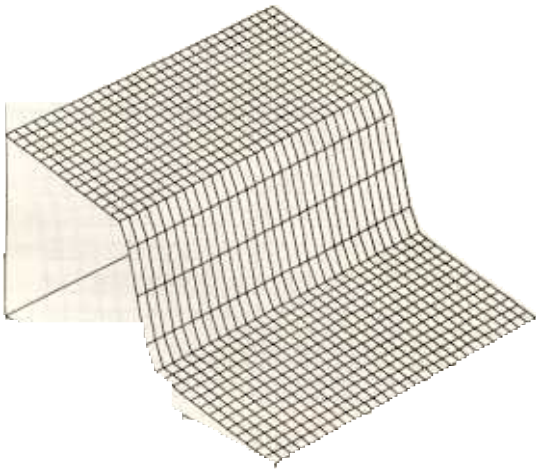
(b)  $\alpha = 0.5, \gamma_{avg} = 0.185$

Figure 8

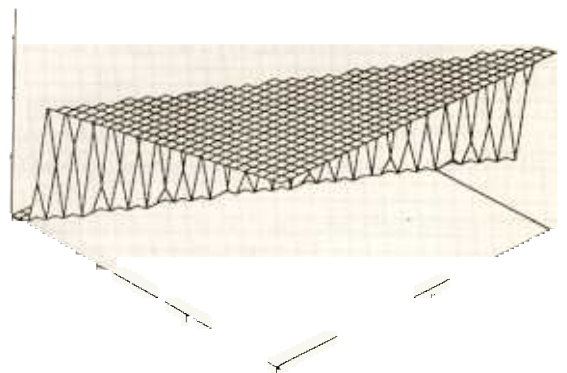
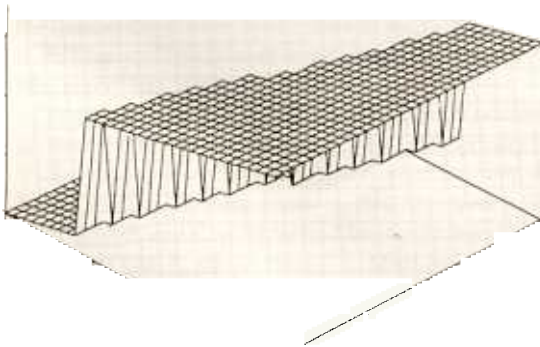


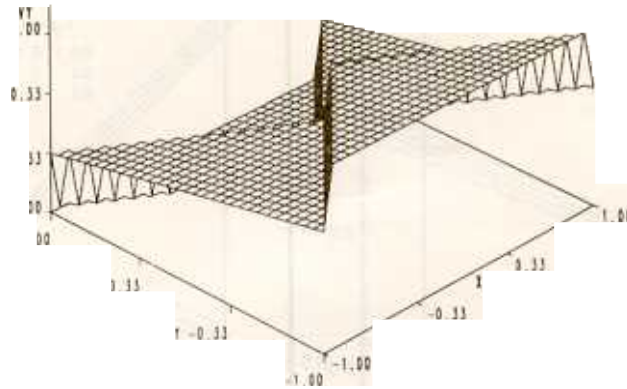
(c) Contours of the dynamic shear strain rate

different values during the late stage of development



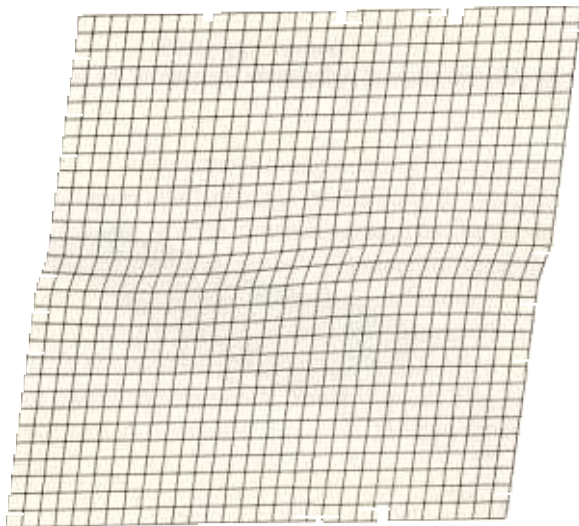
$\dot{\gamma}_{avg}$



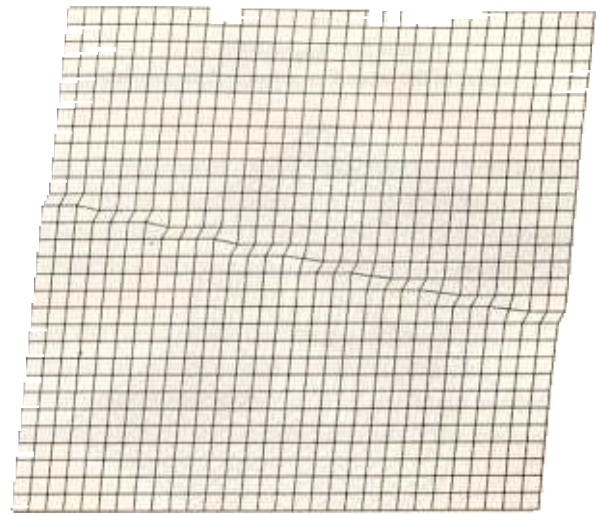


(e)  $\alpha = \infty$ ,  $\gamma_{\text{avg}} = 0.059$

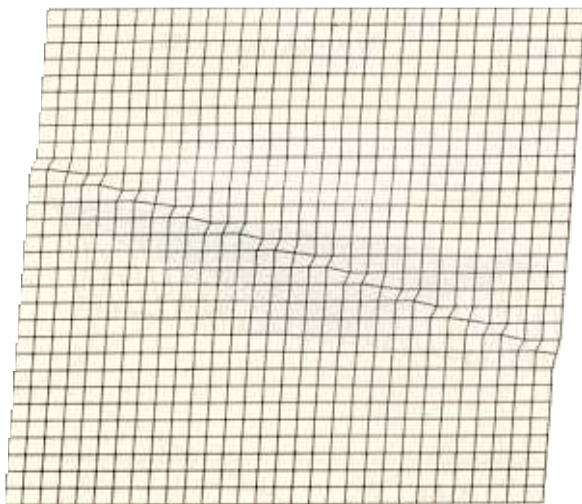
Figure 9. Distribution, at the late stage of the band development, of the y-component of velocity field within the deforming region for  $\alpha = 0.5, 1, 2$  and  $\infty$ , and the x-component of velocity for  $\alpha = 0$ .



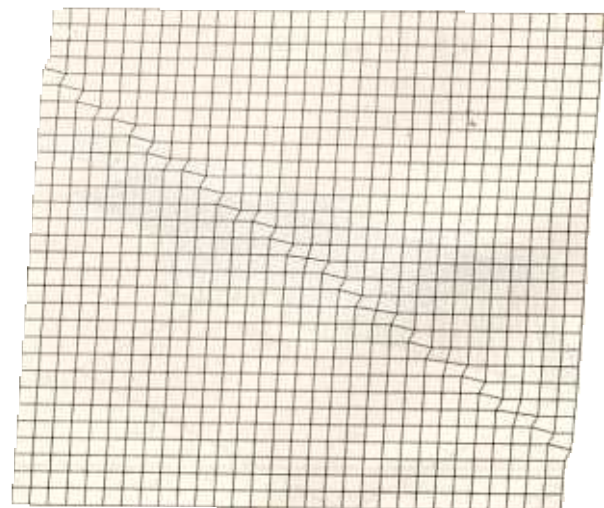
(a)  $\alpha = 0.0$ ,  $\gamma_{\text{avg}} = 0.227$



(b)  $\alpha = 0.5$ ,  $\gamma_{\text{avg}} = 0.185$



(c)  $\alpha = 1.0$ ,  $\gamma_{\text{avg}} = 0.143$



(d)  $\alpha = 2.0$ ,  $\gamma_{\text{avg}} = 0.095$

Figure 10

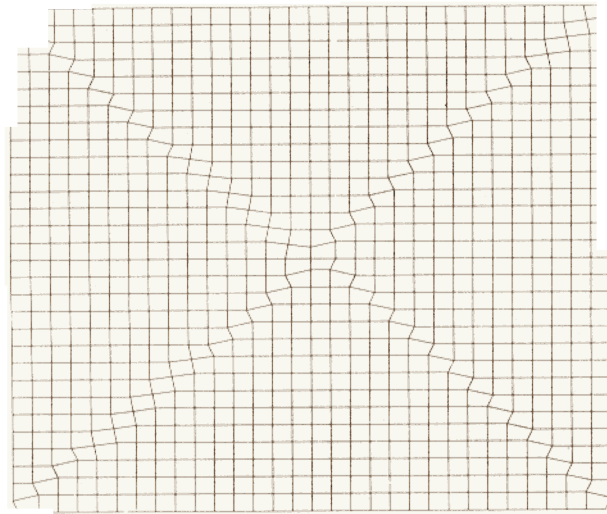
(e)  $\alpha = \infty$ ,  $\gamma_{\text{avg}} = 0.059$ 

Figure 10. Deformed meshes at the late stage of the band development for different loading conditions.

## CONCLUSIONS

We have studied finite plane strain thermomechanical deformations of a thermally softening viscoplastic body of square cross-section and subjected to combined compressive and shearing loads. The material response is modeled by using the Litonski-Batra constitutive relation. A material defect is simulated by assuming that the initial temperature at points surrounding the centroid of the cross-section is higher than that at other points. The higher temperature at and near the centroid softens the material there which is deformed more than the rest of the body. These higher deformations of the material surrounding the centroid of the cross-section heat it up more and the temperature there rises faster than that at other points in the body. The process is self feeding and eventually an instability ensues at the centroid and propagates outwards along the direction of maximum shearing. Because of the rather coarse mesh used, only one element on either side of the band centerline is severely distorted. Also, the deformations within the band are less intense than those computed in the one-dimensional simple shearing problem wherein a fine mesh could be used. One can conclude from the presently computed results that a shear band initiates at the least value of the average strain when the block is deformed in plane strain compression, and the initiation of the band is gradually delayed as the shearing component of deformation is increased.

## ACKNOWLEDGEMENTS

This work was partially supported by the NSF grant MSS9121279 and the U.S. Army Research Office grant DAAL03-91-G-0084 to the University of Missouri-Rolla.

## REFERENCES

1. H. Tresca, On further application of the flow of solids, *Proc. Inst. Mech. Engr.*, **30**, 301-345 (1878).
2. H. F. Massey, The flow of metal during forging, *Proc. Manchester Assoc. Engineers*, pp. 21-26 (1921). Reprinted by the National Machinery Co., Tiffon, OH (1946).
3. C. Zener and J.H. Hollomon, Effect of strain rate on plastic flow of steel, *J. Appl. Phys.*, **14**, 22-32 (1944).
4. B. Dodd and Y. Bai, *Ductile fracture and ductility with applications to metalworking*, Academic Press (1987).
5. Y. Bai and V. Dodd, *Adiabatic shear localization, Occurrence, Theories, and Applications*, Pergamon Press (1992).
6. Y. Bai, Adiabatic shear banding, *Res. Mechanica*, **31**, 133-203 (1990)
7. H.C. Rogers and C.V. Shastry, Material factors in adiabatic shearing in steels, in *Shock Waves and High Strain-Rate Phenomena in Metals*, [M.A. Meyers and L.E. Murr (eds.)], Plenum Press, New York, 285-298 (1981).
8. T.W. Wright and J.W. Walter, On stress collapse in adiabatic shear bands, *J. Mech. Phys. Solids*, **35**, 701-716 (1987).
9. H.M. Zbib and J.S. Jubran, Dynamic shear banding: a three-dimensional analysis, *Int. J. Plasticity*, **8**, 619-641 (1992).
10. R.C. Batra and C.H. Kim, Adiabatic shear banding in elastic-viscoplastic nonpolar and dipolar materials, *Int. J. Plasticity*, **6**, 127-141 (1990).
11. R.C. Batra and C.H. Kim, Effect of viscoplastic flow rules on the initiation and growth of shear bands at high strain rates, *J. Mech. Phys. Solids*, **38**, 859-874 (1990).
12. R.C. Batra and C.H. Kim. Analysis of shear banding in twelve metals. *Int. J. Plasticity*, **8**, 425-452 (1992).

13. Y.M. Wang and R.C. Batra, Effect of kinematic hardening on the initiation and growth of shear bands in plane strain compression of a thermoviscoplastic solid, *Acta Mechanica*, (in press).
14. T.W. Wright and R.C. Batra, The initiation and growth of adiabatic shear bands, *Int. J. Plasticity*, **1**, 205-212 (1985).
15. T.W. Wright and R.C. Batra, Adiabatic shear bands in simple and dipolar plastic materials, in *Proc. IUTAM Symposium on Macro-Micro-Mechanics of High Velocity Deformation and Fracture* [Kawata, K. and Shioiri, J., (eds)], pp. 189-201. Berlin-Heidelberg-New York: Springer (1987).
16. R.C. Batra, The initiation and growth of, and the interaction among adiabatic shear bands in simple and dipolar materials, *Int. J. Plasticity*, **3**, 75-89 (1987).
17. R.C. Batra, Effect of material parameters on the initiation and growth of adiabatic shear bands, *Int. J. Solids and Structures*, **23**, 1435-1446 (1987).
18. R.C. Batra and D.S. Liu, Adiabatic shear banding in plane strain problems, *ASME J. Appl. Mech.*, **56**, 527-534 (1989).
19. R.C. Batra and D.S. Liu, Adiabatic shear banding in dynamic plane strain compression of a viscoplastic material, *Int. J. Plasticity*, **6**, 231-246 (1990).
20. Z.G. Zhu and R.C. Batra, Dynamic shear band development in plane strain compression of a viscoplastic body containing a rigid inclusion, *Acta Mechanica*, **84**, 89-107 (1990).
21. R.C. Batra and X.-T. Zhang, Shear band development in dynamic loading of a viscoplastic cylinder containing two voids, *Acta Mechanica*, **85**, 221-234 (1990).
22. A. Marchand and J. Duffy, An experimental study of the formation process of adiabatic shear bands in a structural steel, *J. Mech. Phys. Solids*, **36**, 251-283 (1988).
23. G.L. Moss, Shear strain, strain rate and temperature changes in an adiabatic shear band, in *Shock Waves and High Strain Rate Phenomenon in Metals*, [Meyer, M.A. and Murr, L.E., (eds)], pp. 299-312, New York, Plenum Press (1981).
24. J. Litonski, Plastic flow of a tube under adiabatic torsion, *Bull. Acad. Pol. Sci.*, **25**, 7 (1977).
25. S.R. Bodner and Y. Partom, Constitutive equations for elastic-viscoplastic strain-hardening materials, *J. Appl. Mech.*, **42**, 385-389 (1975).
26. G.R. Johnson and W.H. Cook, *Proc. Impact Loading and Dynamic Behavior of Materials*, [C.Y. Chiem, H.D. Kunze, and L.W. Mayer (eds.)], Informations gesellschaft, Bremen, FRG (1987).
27. L.S. Costin, E.E. Crisman, R.H. Hawley, and J. Duffy, in *Mechanical Properties at High Strain Rates*, [J. Harding, (ed.)], p. 90, Proc. 2nd Oxford Conf. Inst. Phys., London.
28. R.C. Batra, Steady state penetration of thermoviscoplastic targets, *Computational Mechs.*, **3**, 1-12 (1988).
29. S.B. Brown, K.H. Kim and L. Anand, An internal variable constitutive model for hot working of metals, *Int. J. Plasticity*, **5**, 95-130 (1989).
30. J.F. Bell, *Physics of Large Deformation of Crystalline Solids*, Springer-Verlag, New York (1968).
31. U.S. Lindholm and G.R. Johnson, Strain rate effects in metals at large strain rates, in *Metal Behavior Under High Stresses and Ultrahigh Loading Rates*, [V. Weiss, (ed.)]. Plenum Press, New York, 61-79 (1983).
32. M.L. Lin and R.H. Wagoner, Effect of temperature, strain, and strain-rate on the tensile flow stress of I.F. steel and stainless steel type 310, *Scripta Metallurgica*, **20**, 143-148 (1986).
33. X. Chen and R.C. Batra, Deep Penetration of Thick Thermoviscoplastic Targets by Long Rigid Rods, *Computers and Structures*, (in Press).
34. O.C. Zienkiewicz, E. Onate, and J.C. Heinrich, A general formulation for coupled thermal flow of metals using finite elements, *Int. J. Num. Meth. Engr.*, **17**, 1497 (1981).
35. K.J. Bathe, *Finite element procedures in engineering analysis*, Englewood Cliffs: Prentice-Hall (1982).
36. C. Truesdell and W. Noll, The nonlinear field theories of mechanics, *Handbuch der Physik*, III/3, Springer-Verlag (1965).
37. A. Needleman, Dynamic shear band development in plane strain, *J. Appl. Mechs.*, **56**, 1-9 (1989).
38. C.W. Gear, *Numerical initial value problems in ordinary differential equations*, Englewood Cliffs: Prentice-Hall (1971).
39. A.C. Hindmarsh, ODEPACK, A systematized collection of ODE solvers, in *Scientific Computing*, [Stempleman, R.S. et al., (eds.)], pp. 55-64, Amsterdam: North-Holland (1983).
40. R.C. Batra and K. -I. Ko, An adaptive mesh refinement technique for the analysis of shear bands in plane strain compression of a viscoplastic solid, *Computational Mechs.*, **10**, 369-379 (1992).
41. R.C. Batra and K. -I. Ko, Analysis of shear bands in dynamic axisymmetric compression of a thermoviscoplastic cylinder, *Int. J. Engr. Sci.*, **31**, 529-547 (1993).